IEEE Access
Multidisciplinary | Rapid Review | Open Access Journal

Received 1 April 2024, accepted 14 April 2024, date of publication 17 April 2024, date of current version 26 April 2024.

Digital Object Identifier 10.1109/ACCESS.2024.3390239

RESEARCH ARTICLE

Capacitor Voltage Balancing Based on Improved Carrier Overlapping PWM Method for a Five-Level T-NNPC Converter

HUA CHEN[1], CHUANGPING WEN[2], ZUOHANG HU[2], AND XIANGYANG XING[2], (Member, IEEE)

[1]Department of Electrical Engineering, Shandong Labor Vocational and Technical College, Jinan 250022, China
[2]School of Control Science and Engineering, Shandong University, Jinan 250061, China

Corresponding author: Xiangyang Xing (xyxing@sdu.edu.cn)

This work was supported in part by the National Natural Science Foundation of China under Grant 62222309, Grant 62173210, and Grant 62188101; and in part by the Natural Science Foundation of Shandong under Grant ZR2022JQ29.

ABSTRACT T-NNPC inverter is an attractive topology with fewer switches and good withstand voltage for medium voltage applications. In order to effectively achieve five-level output, the conventional method is an MPC strategy that can quickly track current, ensuring good output performance under fundamental frequency conditions. However, the flying capacitor voltage fluctuates, especially under low-frequency conditions. In addition, the CO-PWM is a potential method for this topology due to the broader voltage level distribution in the vertical direction. Nevertheless, the flying capacitor voltage balancing cannot be guaranteed under the high modulation indexes. To improve voltage balance under various modulation indexes and current frequencies, this paper proposes an improved CO-PWM (ICO-PWM) method whose voltage level distribution is modified to better apply in the T-NNPC topology. Compared to the conventional MPC method, the flying capacitor voltage is more stable, and the fluctuation is reduced by more than five times, especially under low-frequency conditions. The effectiveness of the proposed ICO-PWM method is verified by the simulations and experiments.

INDEX TERMS Multilevel inverter, flying capacitor voltage balancing, carrier overlapping PWM, low current frequency.

I. INTRODUCTION

Multilevel converters have received wide applications in medium-voltage high-power conversions, such as renewable energy conversion and motor drives [1], [2], [3]. As inverter systems develop towards high voltage and high power, the requirements for withstand voltage of the topology structure are gradually increased, and the cost remains a critical factor that cannot be ignored in industrial applications. Multilevel inverters can be mainly divided into the following three categories: neutral-point-clamped (NPC), flying-capacitor (FC), and cascaded H-bridge (CHB) multilevel converters [4], [5], [6]. The development of multilevel inverter topologies based on conventional topologies is rapidly advancing; the increase in the number of levels will increase the number of switches and the size of passive components, resulting in higher costs.

The associate editor coordinating the review of this manuscript and approving it for publication was Inam Nutkani.

As a common topology with multiple levels, the five-level inverter has the above problems.

In order to deal with these limitations, a five-level T-type nested neutral point clamped (T-NNPC) inverter was proposed in [7], which has the main advantages of fewer switches, better voltage withstand performance, and no need for neutral point voltage control. Only the flying capacitor voltage needs to be controlled to output five levels. In [7], A comparison of various related five-level topologies in recent years in terms of the number of switches and flying capacitors, the voltage stress, etc., is provided [8], [9], [10], [11], [12], [13], [14]. Details are shown in Table 1. In addition, some novel topologies are also added to Table 1 [15], [16], [17], [18]. The switched-capacitor topology is an attractive topology in recent years for substituting the two-stage structure due to its voltage boost ability [16], [17], [18]. The flying capacitors of this topology are naturally balanced. However, the maximum current stress in this topology is

more significant than that in other topologies. The concrete comparison of this topology and the T-NNPC is given in Table 1.

In addition, It can be seen from Table 1 that the T-NNPC topology has the fewest number of switches, the lower total withstand voltage, no need for neutral point voltage balancing control, a more straightforward algorithm design, and fewer passive components. Although the T-NNPC topology has several advantages mentioned above, the design of the flying capacitor voltage control method is a challenge. The conventional sinusoidal PWM (SPWM) method in [19] and [20], such as phase disposition PWM (PDPWM) and phase shifted PWM (PSPWM), cannot be applied to the T-NNPC topology, so a more flexible MPC method is used to achieve five-level output in [7]. However, the flying capacitor voltage control is controlled by a weight factor, which requires extensive testing and is an empirical value, making it more complex [21]. Moreover, insufficient redundancy of the flying capacitor voltage further increases the complexity of the flying capacitor voltage control.

The carrier overlapping PWM (CO-PWM) method is a potential modulation method to realize the flying capacitor voltage control of the T-NNPC topology of its unique voltage level distribution from conventional SPWM [22]. The voltage level distribution in the CO-PWM is more suitable for the flying capacitor voltage control of the T-NNPC topology. Compared with conventional SPWM methods, the voltage level of CO-PWM is higher in the vertical direction than that of conventional SPWM methods. Therefore, based on the conventional CO-PWM method, an improved CO-PWM (ICO-PWM) strategy is proposed in this paper to further expand the distribution of voltage levels in the vertical direction, which can effectively suppress the fluctuation of the flying capacitor voltage, both in low frequency and high modulation index conditions, with rapid dynamic response and no significant fluctuation.

In this paper, in order to ensure the flying capacitor balancing under different conditions, an improved CO-WPM method is proposed for the T-NNPC topology. The main innovation of this article lies in

1) The ICO-PWM method solves the problem that the conventional SPWM methods cannot effectively control the voltage of flying capacitors under high modulation indexes. Based on expanding the voltage level distribution in the vertical direction, the voltage level contents for controlling the flying capacitors are increased, thus achieving good five-level output through modulation strategies in the T-NNPC topology.

2) Compared to the conventional MPC method, the ICO-PWM improves the stability of flying capacitor voltage control under low-frequency conditions, reduces the flying capacitor voltage deviation by more than five times, and improves the performance of output current.

The rest of this article is organized as follows. In Section II, the operation principle of T-NNPC topology is explained briefly. The mathematical model is obtained in the Section III.

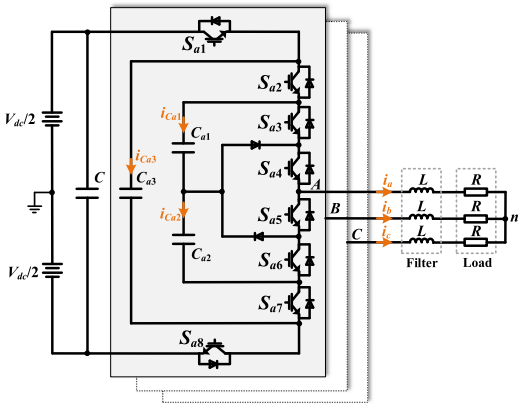

FIGURE 1. Topology of the 5L-NNPC inverter.

The principle of conventional MPC method and the proposed ICO-PWM method are explained in Section IV. The steady-state and dynamic results of experiments are given in Section V.

II. TOPOLOGY AND ITS OPERATION PRINCIPLE

As shown in Fig. 1, the 5L-NNPC topology consists of three flying capacitors $C_{xj}(x = a, b, c$ and $j = 1, 2, 3)$ and eight power switches (S_{x1}, S_{x2}, S_{x3}, S_{x4}, S_{x5}, S_{x6}, S_{x7} and S_{x8}) for each phase and a common DC-link voltage source without the DC-link neutral point. As shown in Fig. 2, the T-NNPC topology is simplified based on the 5L-NNPC topology, which requires less number of flying capacitors and power switches. The DC-link voltage is defined as V_{dc} and the DC-link capacitor is defined as C. To ensure equally spaced steps in the output voltages, both the flying capacitors C_{x1} and C_{x2} are charged to $V_{dc}/4$. The output phase voltages are V_a, V_b and V_c, respectively. The output phase currents are i_a, i_b, and i_c, respectively. i_{Cxj} represents the flying capacitor current. The output side for each phase is connected with an inductance L and a resistance R. n denotes the output neutral point.

Five output levels are achieved from twelve distinct switching states in the 5L-NNPC inverter, while the T-NNPC inverter only has six distinct switching states. So there are less choices for the T-NNPC inverter to control the flying capacitor voltages. Table 2 gives the switching state and its corresponding flying capacitor voltage control of the T-NNPC inverter. Fig. 3 shows the switching state and its corresponding switching conduction state.

It can be observed from the Table 2 and Fig. 3 that only the voltage level "0.5 V_{dc}" among the five level voltages has two redundant switching states. It is seen that the switch state $0.5V_{dc(1)}$ will charge the flying capacitor and increase the flying capacitor voltage, on the contrary, the switch state $0.5V_{dc(2)}$ will discharge the flying capacitor and decrease the flying capacitor. Thus, the two switching combinations mentioned above are utilized to control the flying capacitor voltage. Moreover, the flying capacitor voltages of V_{Cx1} and

TABLE 1. Comparison of derived topologies.

Topologies	Number of Switches	Number of diodes	Number of neutral points	Number of FCs	Switching voltage stress (V_{dc})	Total voltage stress (V_{dc})	Maximum current stress	DC-link voltage (V_{dc})	Voltage boost ability
5L-ANPC [8]	24	24	1	3	1/2 or 1/4	9	I_p	1	no
New 5L-ANPC [9]	36	36	1	9	1/4	9	I_p	1	no
7S-5L-ANPC [10]	27	33	1	3	3/4, 1/2 or1/4	9.5	I_p	1	no
5L-NNPC [11], [12]	18	24	0	6	1/2 or 1/4	7.5	I_p	1	no
5L-FC-NNPC [13]	24	30	6	15	1/4	6	I_p	1	no
5L-HC [14]	30	30	2	6	1/2 or 1/4	7.5	I_p	1	no
6S-5L-ANPC [15]	18	18	1	3	3/4, 1/2 or1/4	9	I_p	1	no
ABNPC [16]	18	18	1	3	1/2 or 1/4	7.5	$>I_p$	1/2	yes
SCANPC [17]	24	24	1	3	1/2 or 1/4	7.5	$>I_p$	1/2	yes
T-NNPC	**18**	**18**	**0**	**6**	**1/2 or 1/4**	**7.5**	I_p	**1**	**no**

I_p: peak value of output current.

TABLE 2. Switching states and its corresponding flying capacitor voltage control of T-NNPC topology.

S_{x1}	S_{x2}	S_{x3}	S_{x4}	S_{x5}	S_{x6}	V_{ref}	ΔV_{cx1}	ΔV_{cx2}
1	1	0	0	0	0	V_{dc}	0	0
1	0	0	0	1	1	$0.75V_{dc}$	+	0
1	0	1	0	0	0	$0.5V_{dc(1)}$	+	+
0	1	0	1	0	0	$0.5V_{dc(2)}$	-	-
0	0	0	1	1	1	$0.25V_{dc}$	0	-
0	0	1	1	0	0	0	0	0

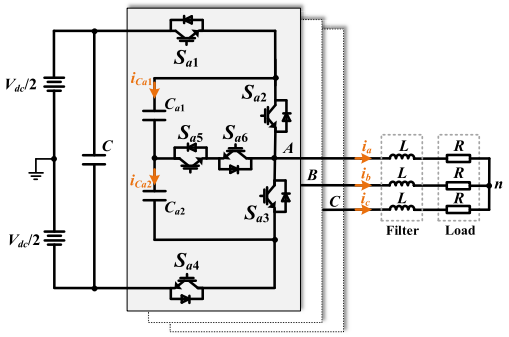

FIGURE 2. Topology of the 5L-T-NNPC inverter.

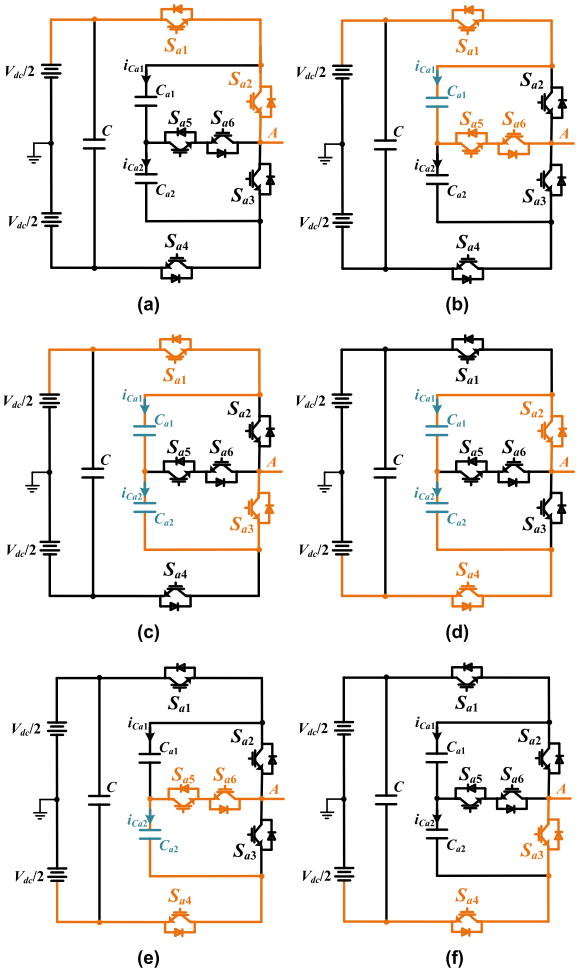

FIGURE 3. Switching states of the T-NNPC inverter. (a) V_{dc}, (b) $0.75V_{dc}$, (c) $0.5V_{dc(1)}$, (d) $0.5V_{dc(2)}$, (e) $0.25V_{dc}$ and (f) 0.

V_{Cx2} are coupled since the voltage are only controlled by changing the switching states in the voltage level "0.5 V_{dc}".

III. MATHEMATICAL MODEL OF THE INVERTER SYSTEMS

In this section, according to the circuit of the T-NNPC topology shown in Fig. 2, the output currents and FC voltages are obtained based on the Kirchhoff's voltage and current law.

The output load currents can be expressed as

$$V_{xN} = L\frac{di_x}{dt} + Ri_x + V_{nN}, \quad x = a, b, c \tag{1}$$

where V_{xN} is the output phase voltage with respect to the negative side of dc-link voltage (N).

As shown in Fig. 2, according to the Kirchhoff's law of voltage (KVL), the output phase voltage equations of the T-NNPC topology can be written as

$$V_{xn} = V_{xN} - V_{nN} = L\frac{di_x}{dt} + Ri_x, \quad x = a, b, c \tag{2}$$

According to the Kirchhoff's law of current (KCL), the output currents are expressed as

$$i_a + i_b + i_c = 0 \tag{3}$$

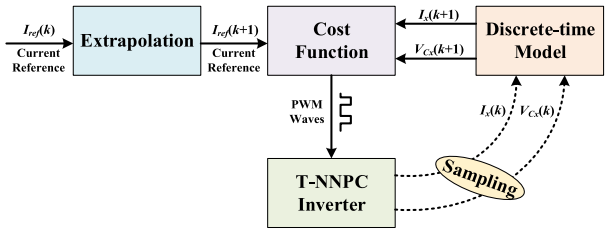

FIGURE 4. Control block diagram of MPC method for the T-NNPC inverter.

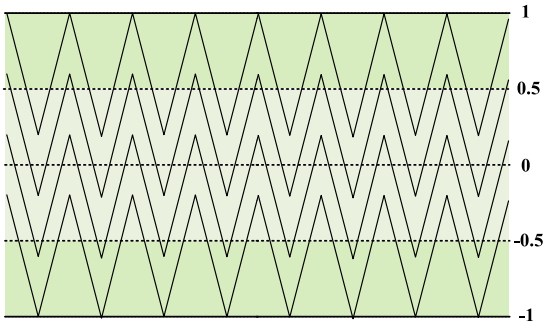

FIGURE 5. Carrier waveform of Conventional CO-PWM.

Based on the relationship between capacitor voltage and current, the FC current can be expressed as

$$i_{Cxj} = C_{xj}\frac{dV_{Cxj}}{dt}, \quad x = a, b, c\&j = 1, 2 \tag{4}$$

where V_{cx1} and V_{cx2} are the voltage of C_{x1} and C_{x2}.

IV. THE CONVENTIONAL METHODS AND IMPROVED CO-PWM METHOD

A. CONVENTIONAL METHODS

The FCS-MPC has been widely applied in power electronics due to its capability to control diverse objects and the existence of an accurate mathematical model of the power converters. Based on the advantages of FCS-MPC method, an MPC method for T-NNPC is used in [7], and the control block diagram is shown in Fig. 4, where the $I_x(k)$ and $V_{Cx}(k)$ are the output currents and flying capacitor voltages in the kth instant, the $I_x(k+1)$, $V_{Cx}(k+1)$ are the output currents and flying capacitor voltages in the $k+1$th instant.

In FCS-MPC method for the T-NNPC topology, the flying capacitor voltage is controlled by weighting factors, but due to the complexity of selecting weighting factors, the control stability of the flying capacitor voltage is poor when using a single vector. For this type of topology, the essential target is the stability of the flying capacitor voltage. Otherwise, the five-level output phase voltage cannot be effectively guaranteed.

For multi-level inverter systems, one of the typical methods is the SPWM strategy, but this method cannot be directly applied to this topology. The T-NNPC topology only has two switching states to control the flying capacitor voltage, so the conventional SPWM method can only control the flying capacitor voltage under a low modulation index. As shown in Fig. 5, the conventional five-level CO-PWM uses four carriers with the same frequency and amplitude, evenly distributed within the modulation range. Based on the conventional phase disposition PWM (PDPWM) method, the conventional CO-PWM method shifts the carrier in the vertical direction and changes the amplitude of the carrier. The conventional CO-PWM method has good harmonic performance under a low modulation index, and it is basically the same as the specific harmonic elimination PWM (SHEPWM) method under a high modulation index. In addition, the voltage level distribution of the CO-PWM method is wider in the vertical direction compared to the PDPWM method, and the range of flying capacitor voltage control is also larger. However, it is unable to control the flying capacitor voltage within the whole modulation index.

B. IMPROVED CO-PWM METHOD

In order to effectively control the flying capacitor voltage under a high modulation index, it is necessary to modify the conventional CO-PWM method. Therefore, this paper proposes an improved CO-PWM method.

Based on the analysis of the conventional method, as shown in Fig. 7, the amplitude of the carrier waveform in the ICO-PWM method is modified, the average amplitude of the four carriers is 1, and the carriers are not evenly distributed. It can be seen that the amplitude of the carrier can be changed according to the performance of the flying capacitor voltage control and the DC voltage utilization. In addition, g is defined as the carrier amplitude adjustment factor. After introducing g, the amplitudes of carrier C_{r1} and C_{r4} become 1-g, while the amplitudes of carrier C_{r2} and C_{r3} become 1+g. Therefore, the carrier ranges of the voltage levels "V_{dc}", "$0.75V_{dc}$", "$0.5V_{dc}$", "$0.25V_{dc}$" and "0" in the vertical direction of the proposed method is 1-g, 1+g, 2, 1+g and 1-g, respectively. Different carrier amplitude adjustment factors produce different output performance with a particular range. If g is too high, it can lead to distortion in the output current and even cause unstable voltage control of flying capacitors and a decrease in DC voltage utilization. If g is too low, the output voltage is almost the same as that of the three-level inverter, and the advantage of the T-NNPC topology is no longer existent. In order to effectively control the flying capacitor voltage and ensure the performance of the output current, it is necessary to adjust the position of the carriers to generate the voltage level that controls the flying capacitor voltage in each carrier range.

Fig. 8 shows the voltage level distribution of the ICO-PWM method. Compared to Fig.8 and Fig. 6, it can be observed that the carrier ranges of the voltage levels "V_{dc}", "0.75 V_{dc}", "0.25 V_{dc}" and "0" in the vertical direction in the ICO-PWM method are similar to that in the conventional CO-PWM method. However, the carrier range of the voltage level "0.5 V_{dc}" in the vertical direction in the ICO-PWM method is obviously greater than that in the conventional

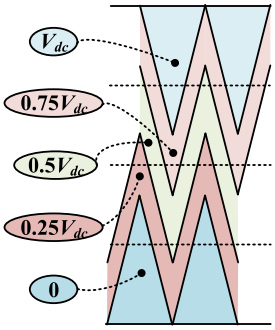

FIGURE 6. Voltage level distribution of conventional CO-PWM.

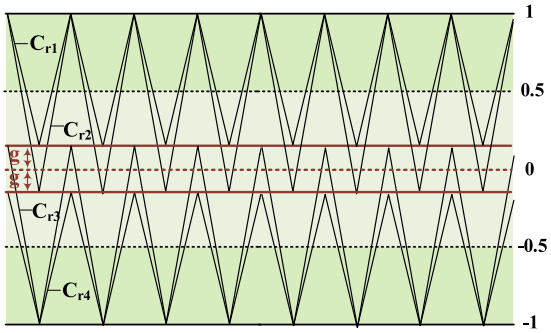

FIGURE 7. Carrier waveform of ICO-PWM.

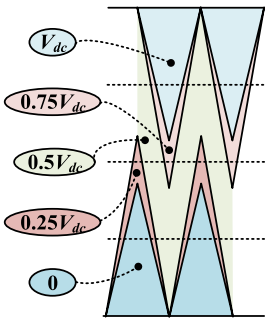

FIGURE 8. Voltage level distribution of ICO-PWM.

CO-PWM method. The voltage level "0.5 V_{dc}" can cover the whole vertical direction, which benefits the flying capacitor voltage control. Table 3 gives the percentage compositions of the different voltage levels in the vertical direction, which is the proportion of the voltage level in the vertical direction over the entire carrier range. Obviously, the voltage level "0.5 V_{dc}" in the ICO-PWM method is greater than that in the CO-PWM method. The average percentage composition of other voltage levels in the ICO-PWM method are the same to that in the CO-PWM method, which is 50%.

Based on the previous analysis of the carrier amplitude adjustment factors g, Fig. 9 shows the voltage level distributions of ICO-PWM under $g = 0.05$, 0.25, and 0.15.

i) When $g = 0.05$, the contents of "0.75 V_{dc}", "0.25 V_{dc}" are low, the voltage levels almost change among "V_{dc}", "0.5 V_{dc}", and "0" in the low modulation indexes, leading to large

TABLE 3. Percentage compositions of the different voltage levels in vertical direction.

method		CO-PWM	ICO-PWM				
g		-	0.05	0.15	0.2	0.25	0.30
Percentage composition (%)	V_{dc}	40	47.5	42.5	40	37.5	35
	$0.75V_{dc}$	60	52.5	57.5	60	62.5	65
	$0.5V_{dc}$	60	100	100	100	100	100
	$0.25V_{dc}$	60	52.5	57.5	60	62.5	65
	0	40	47.5	42.5	40	37.5	35

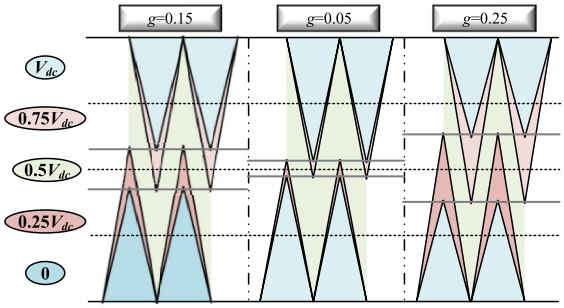

FIGURE 9. Voltage level distributions of ICO-PWM under different carrier amplitude adjustment factors.

THD of output current in the low modulation indexes. When g is lower than 0.05, the output phase voltage in this condition is similar to that in a three-level inverter, so the advantages of the topology no longer exist. Combined with the simulation diagram, it can also be seen from Fig. 10(a) that the output phase voltage is similar to a three-level inverter, and the output line voltage is similar to a five-level inverter.

ii) When $g = 0.25$, the contents of "0.75 V_{dc}", "0.25 V_{dc}" are high, and the content of "0" gradually decreases. When g is higher than 0.25, the ability of flying capacitor voltage control decreases, and the output current begins to distort, which is not conducive to the stable operation of the system. Combined with the simulation diagram, it can be seen that when $g = 0.25$, the deviation of flying capacitor voltage is larger than other conditions. As shown in Fig. 10(d), the deviation of flying capacitor voltage under $g = 0.4$ is obvious, the current distortion is serious, and the THD is the highest.

iii) When $g = 0.15$, as shown in Fig. 10(c), the distribution of various voltage levels is uniform, the flying capacitor voltage control is stable, and the output performance is good.

Therefore, according to the simulation result under different values of g, the range of g is taken to be 0.05∼0.25 in this paper, and 0.15 is used as the parameter for simulation and experiments.

C. CONTROL BLOCK DIAGRAM

Fig.11 shows the control block diagram of the ICO-PWM method for the T-NNPC topology. Among that, the flying capacitor voltage control is given. The flying capacitor voltage control function can be written as

$$ConV_{Cxj} = (V_{Cxj} - V_{dc}/4) * i_x, \quad x = a, b, c \& j = 1, 2 \quad (5)$$

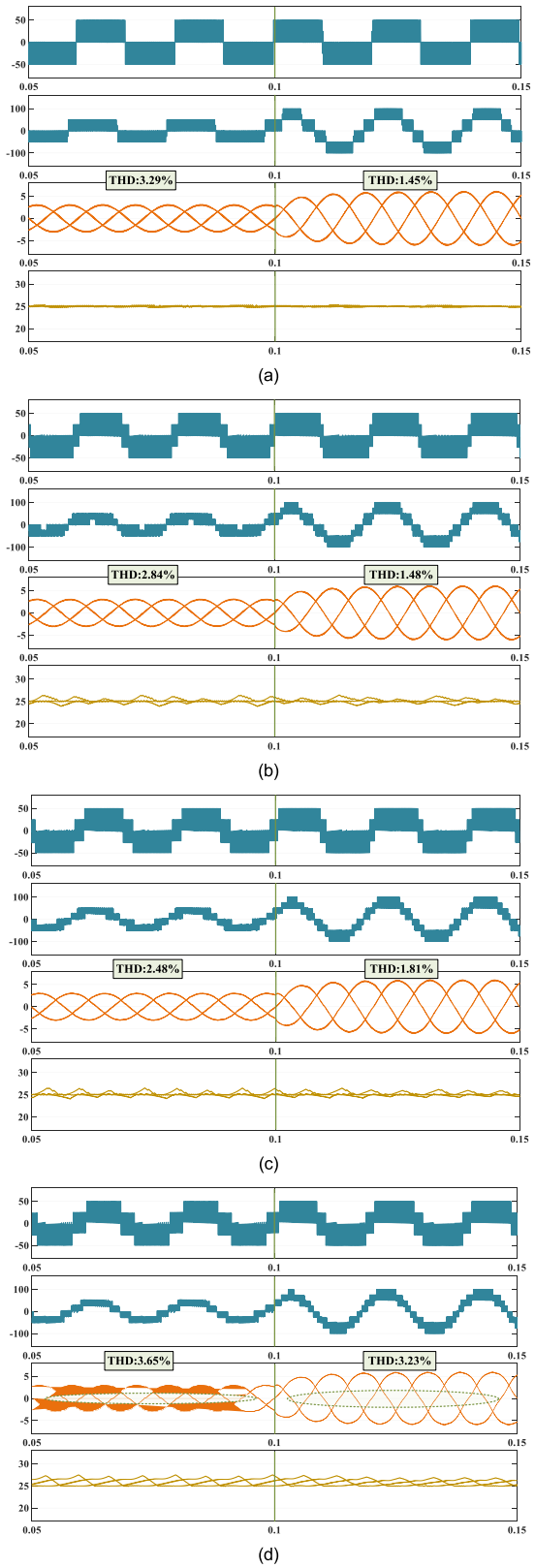

FIGURE 10. Simulation results under different carrier amplitude adjustment factors when the current reference changes from 3 A to 6 A, including phase voltage (V_a), line voltage (V_{ab}), output current (i_a) and its THD, and flying capacitor voltage of C_{x1} (V_{Cx1}). (a) $g = 0.05$, (b) $g = 0.15$, (c) $g = 0.25$, and (d) $g = 0.4$.

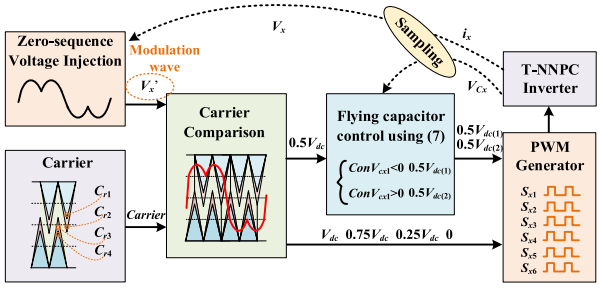

FIGURE 11. Control block diagram of the proposed ICO-PWM method for the T-NNPC topology.

Due to the particularity of the T-NNPC topology, two flying capacitors are connected in series, and their control is coupled. So, the flying capacitor voltages are controlled by changing the redundant switching states at the voltage level of "0.5 V_{dc}". The flying capacitor control can be mainly summarized into the following two cases:

1) When the voltage levels are "V_{dc}", "0.75 V_{dc}", "0.25 V_{dc}", and "0", there is no redundancy state. In this case, no flying capacitor voltage control.

2) When the voltage level is "0.5 V_{dc}", there are two redundant states in this voltage level, and the redundant states have opposite effects on charging and discharging the flying capacitor voltage, thus meeting the requirements for controlling the flying capacitor voltage. In this way, by sampling the voltage deviation of the flying capacitor and the direction of output current, the corresponding switching combinations are selected. For example, when $(V_{ca1}\text{-}V_{dc}/4)>0$, which means the phase-A voltage of flying capacitor voltage is higher than the required values and need to be decreased if the output current i_a is positive, so the $0.5V_{dc(2)}$ state will be adopted to reduce the flying capacitor voltage. Therefore, it is necessary to add the content of the voltage level "0.5 V_{dc}" for the stability of the flying capacitor voltage.

It should be noted that in order to ensure the utilization rate of SPWM, a zero-sequence voltage is injected into the modulated wave. The remaining modules in the control block diagram are the same as conventional SPWM methods.

V. SIMULATION RESULTS

Due to the inconsistency in the switching frequencies commonly used in conventional MPC method and the proposed method, a comparative analysis of the output effects of the two methods at their respective switching frequencies was conducted. The parameters of the simulation and experiments are given in Table 4.

For more fair comparison, a comparative analysis of the proposed method and conventional MPC methods under two switching frequencies are conducted, one is the low switching frequency of 4 kHz for conventional MPC, the other is the high switching frequency of 12 kHz for the proposed method. Here, the average switching frequency is calculated by the

TABLE 4. Experimental parameters.

Parameters	Value
DC-link voltage (V_{dc})	100 V
Current Reference(i_d)	3 / 6 A
Current frequency (f_c)	10 / 50 /100 Hz
DC-side capacitor (C)	2350 μF
Resistance (R)	8 Ω
Filter inductor (L)	3 mH
Flying capacitors (C_{x1}, C_{x2})	2350 μF, 2350 μF
Line frequency (f_{line})	50 Hz
Carrier amplitude adjustment factors (g)	0.15
Switching frequency	4 kHz/12 kHz
Control period (T_s)	200 μs

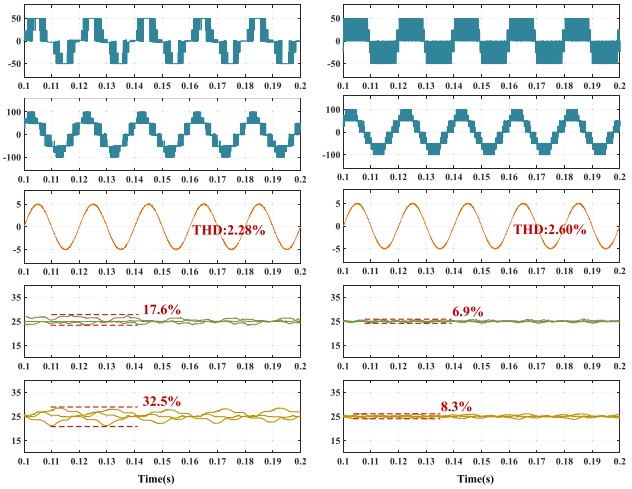

FIGURE 12. Output waveforms of the conventional MPC method and the proposed method when the switching frequency is 4 KHz, including phase voltage (V_{an}), line voltage (V_{ab}), output current (i_a), voltage of C_{x1} and C_{x2} (V_{Cx1} and V_{Cx2}).

PWM waveforms of each switch in MATLAB/Simulink. Fig. 12 shows the output waveforms of the two methods under the low switching frequency of 4 kHz, including phase voltage (V_{an}), line voltage (V_{ab}), output current (i_a), voltage of C_{x1} and C_{x2} (V_{Cx1} and V_{Cx2}). It can be seen that the proposed method can also operate stably at 4 kHz. At this switching frequency, the output current THD of the proposed method is slightly lower than that of conventional MPC method. However, in terms of flying capacitor voltage control, the proposed method is significantly better than conventional MPC method. The flying capacitor voltage of the proposed method is controlled within 10%, maintaining good stability, while the flying capacitor voltage fluctuation of conventional MPC method is large and frequent, with fluctuation of V_{Cx2} exceeding 30%.

In addition, Fig. 13 shows the output waveforms of the two methods under the high switching frequency of 12 kHz. It can be seen that the output current THD of the proposed method is basically the same as that of conventional MPC method,

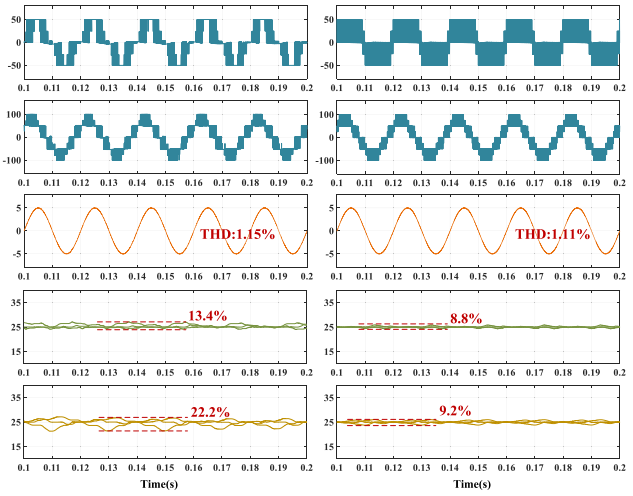

FIGURE 13. Output waveforms of the conventional MPC method and the proposed method when the switching frequency is 12 KHz, including phase voltage (V_{an}), line voltage (V_{ab}), output current (i_a), voltage of C_{x1} and C_{x2} (V_{Cx1} and V_{Cx2}).

while the flying capacitor voltage control is also better than conventional MPC method, with the flying capacitor voltage fluctuation controlled within 10%. It can be concluded that the proposed method has advantages in flying capacitor voltage control and the voltage stress of each switch avoid rising significantly from the frequent fluctuations in flying capacitor voltage, which can ensure system stability. It should be pointed out that the voltage levels "$0.25V_{dc}$" and "$0.75V_{dc}$" also have an impact on the flying capacitor voltage control. Therefore, it can be seen from Fig. 12 and 13 that the instability of the flying capacitor voltage control in the conventional MPC method leads to the large fluctuation difference of the flying capacitor voltages. While the fluctuation difference of the flying capacitor voltages in the ICO-PWM method is small due to the better flying capacitor voltage control.

In order to better demonstrate that the proposed method can produce better output current than the conventional MPC method under the same conditions, the THD of output current under different modulation indexes is compared, as shown in Fig. 14. It can be seen that both methods can meet the standard for output current THD of inverters in the given range of modulation indexes. The proposed ICO-PWM method is superior to the MPC method under all modulation indexes. In addition, the MPC method is unstable when the modulation indexes are higher than 0.9, resulting in output current distortion and increased current THD. The proposed ICO-PWM method can produce a stable output current under all modulation indexes, which is in line with the general rule that the output current THD decreases as the modulation index increases.

VI. EXPERIMENTAL RESULTS

The simulation results provide comparison of output waveforms under the same switching frequency. In order to better compare the output performance of the proposed method and

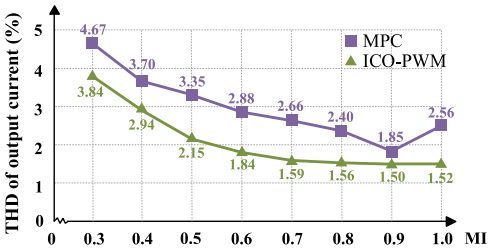

FIGURE 14. Comparison of THD of output current under the MPC and ICO-PWM methods.

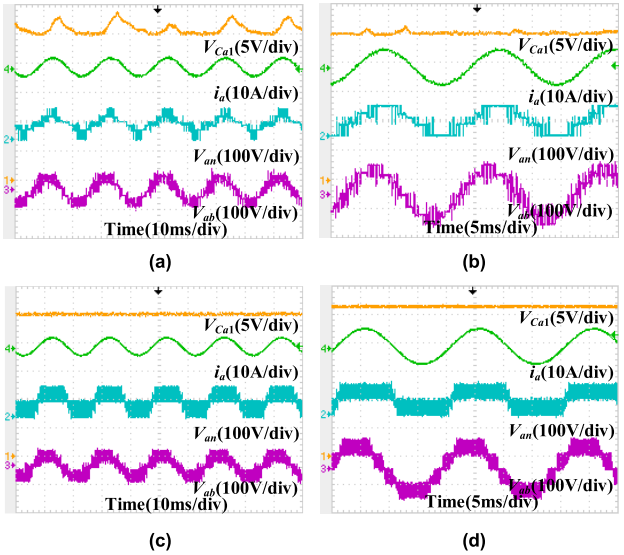

FIGURE 15. Comparison of the MPC and ICO-PWM method under f_c = 50 Hz. (a) MPC under i_d = 3 A, (b) MPC under i_d = 6 A, (c) ICO-PWM under i_d = 3 A, and (d) ICO-PWM under i_d = 6 A.

conventional MPC method under their respective frequencies, the experiments utilize their commonly used switching frequencies. Based on the comparative analysis of conventional methods and the ICO-PWM method, in this section, experimental verification and analysis are conducted on the conventional MPC method in [7] and the ICO-PWM method using experimental equipment. The experimental results under different conditions are compared. The comparison of steady-state results includes high and low modulation indexes, high and low modulation under low-frequency conditions. The comparison of the transient results includes current reference change, current frequency changing from low frequency to fundamental frequency, and from fundamental frequency to high frequency. The advantages of the proposed method compared to the MPC methods, the stability of flying capacitor voltage, the output current ripple, etc., were analyzed under different conditions. It should be pointed out that in order to more clearly compare the difference between the proposed ICO-PWM method and the conventional MPC method under low-frequency conditions, a lower sampling frequency is adopted in this paper.

The modulation index is adjusted by changing the current reference (3 A/ 6 A). According to [23], the modulation index is calculated as

$$\mathrm{MI} = \frac{\sqrt{3}\, i_d \cdot R}{V_{dc}} \tag{6}$$

where MI is the modulation index, i_d is the current reference.

According to (6), when the current reference is 3 A, the modulation index is calculated as 0.416, which represents the condition of low modulation index in this paper. Similarly, when the current reference is 6 A, the modulation index is calculated as 0.831, which represents the condition of high modulation index.

A. STEADY-STATE RESULTS

Fig. 15 shows the output performance of MPC and ICO-PWM methods under the fundamental frequency condition with current references of 3 and 6 A, including the performance of flying capacitor voltage, output current, phase voltage, and line voltage. As given in Fig. 15(a) and (b), when the current reference is 3 A, the voltage fluctuation of the MPC is close to 4 V, with a fluctuation ratio of 16%. When the current reference is 6 A, the fluctuation of the MPC is around 1 V, with a fluctuation ratio of 4%. In both modulation indexes, the fluctuation of the MPC method is relatively frequent, which is not conducive to the stability of the system. However, it can be seen from Fig. 15(c) and (d) that the ICO-PWM method has a stable flying capacitor voltage of 25V, with no significant fluctuation in the experimental figure (5V/div), which is superior to the MPC method. Other output waveforms in the ICO-PWM method perform better than those in the MPC method since the flying capacitor voltage is well-controlled in the ICO-PWM method. Therefore, it is proved that the stability of the flying capacitor voltage is the key to the stability of the T-NNPC inverter.

The stability of the flying capacitor voltage control under the fundamental frequency in the ICO-PWM method has a good performance. However, for flying capacitor inverters, the control of flying capacitors under low frequency is a challenge that determines the application of this topology. Fig. 16 shows the output performance of MPC and ICO-PWM methods under the low-frequency condition of 10 Hz. In this condition, the deviation of the flying capacitor voltage under i_d = 3 A is around 10 V, with a fluctuation ratio of 40%, which exceeds the standard for voltage deviation of flying capacitor. Meanwhile, the output phase voltage and line voltage obviously distort. The flying capacitor voltage control under the low frequency in the MPC method is unstable, while the flying capacitor voltage in the ICO-PWM method is well controlled, which is basically consistent with that under the fundamental frequency.

In addition, to prove the ability of the proposed ICO-PWM method and the conventional CO-PWM method to balance the flying capacitor voltage, the flying capacitor voltage ripple with various modulation indexes and power factors is shown in Fig. 17. It is seen from Fig. 17(a) that in

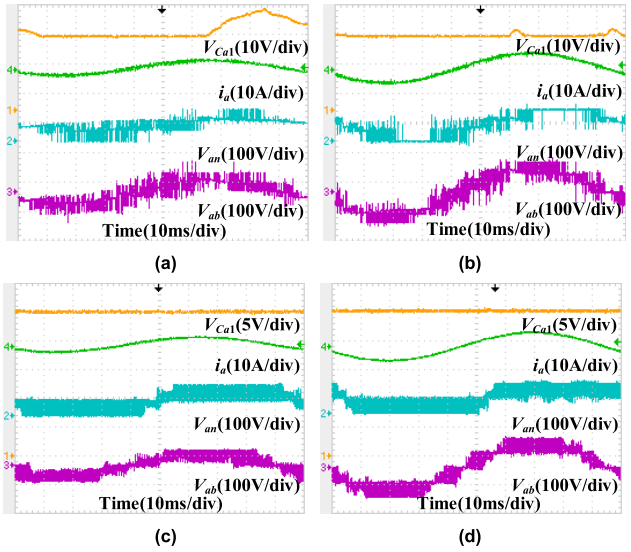

FIGURE 16. Comparison of the MPC and ICO-PWM method under f_c = 10 Hz. (a) MPC under i_d = 3 A, (b) MPC under i_d = 6 A, (c) ICO-PWM under i_d = 3 A, and (d) ICO-PWM under i_d = 6 A.

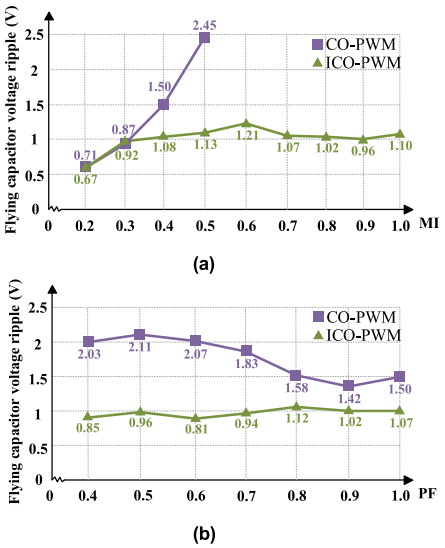

FIGURE 17. Measurement results of the flying capacitor voltage ripple in the two methods under the different conditions. (a) Measurement result of voltage ripple with different modulation indexes. (b) Measurement result of voltage ripple with different power factors.

low modulation indexes, both methods can achieve flying capacitor voltage balance. However, the voltage ripple of the proposed ICO-PWM method is smaller than that of conventional CO-PWM method. When the modulation index is greater than 0.5, the conventional CO-PWM method cannot balance the flying capacitor voltage, while the proposed method can still control the flying capacitor voltage effectively.

Fig. 17(b) is conducted when the output current reference is 3A. As shown in Fig. 17(b), both the methods can control the flying capacitor voltage in different power factors since the modulation index is low. Nevertheless, the voltage ripple of

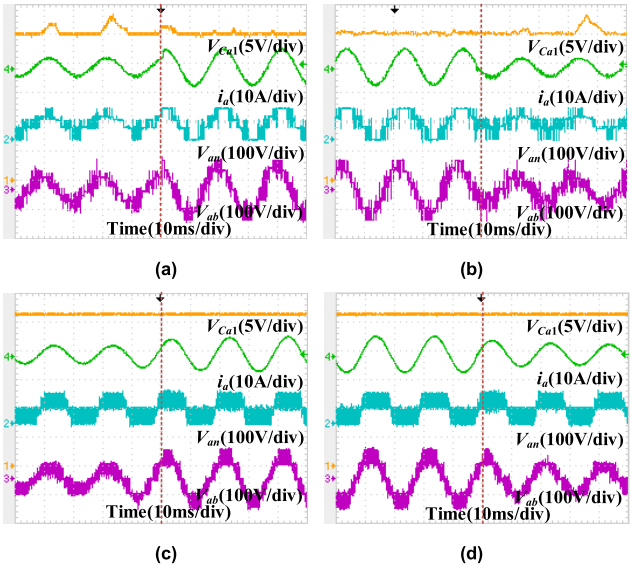

FIGURE 18. Dynamic results of the MPC and ICO-PWM method under changing current reference. (a)/(c) MPC /ICO-PWM under the current reference changing from 3 to 6 A, (b)/(d) MPC /ICO-PWM under the current reference changing from 6 to 3 A.

the proposed ICO-PWM method is smaller than that of conventional CO-PWM method in the full power factor range.

B. DYNAMIC RESULTS

Fig. 18 shows the output performance of MPC and ICO-PWM methods under changing the current references from 3 to 6 A. It can be seen that the fluctuation of flying capacitor voltage in the MPC method is higher than that in the ICO-PWM method, which conforms to the analysis in the steady-state results. In the ICO-PWM method, the output response is quick and the flying capacitor voltage does not fluctuate under the transient condition of the current reference.

In order to further verify the stability of the flying capacitor voltage control in the ICO-PWM method, the experiments for frequencies ranging from 10 Hz, 50 Hz, and 100 Hz are conducted, as shown in Fig. 19 and Fig. 20. The dynamic responses of both methods under the current frequency variation are fast. However, the output performance in the ICO-PWM method is better than that in the MPC method. Consistent with the previous analysis, the greater the fluctuation of the flying capacitor voltage, the more obvious the distortion of the output phase voltage and line voltage, and the output current THD also increases accordingly. It can be seen that in the proposed ICO-PWM method, the flying capacitor voltage can maintain good stability regardless of frequency changes, which is of great significance for the application of this topology. Better control of the flying capacitor voltage can also reduce the number and volume of passive components. The conventional MPC method requires more flying capacitors and inductors, while under the proposed method, less number and volume of flying capacitors and inductors

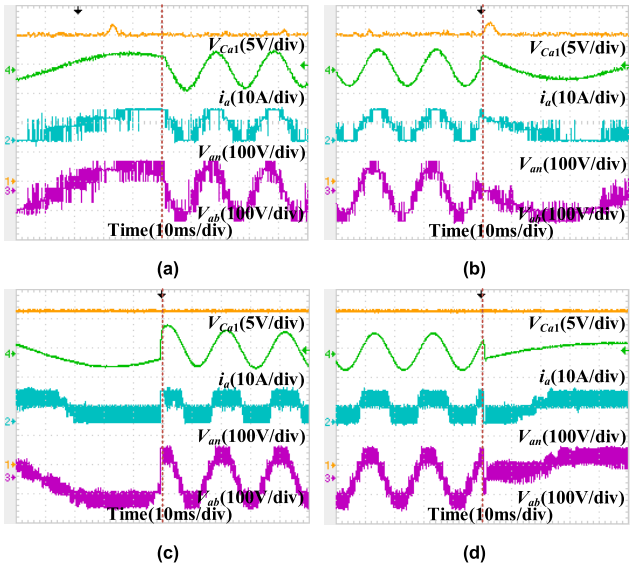

FIGURE 19. Dynamic results of the MPC and ICO-PWM method under changing current frequency. (a)/(c) MPC /ICO-PWM under the current frequency changing from 10 to 50 Hz, (b)/(d) MPC /ICO-PWM under the current frequency changing from 50 to 10 Hz.

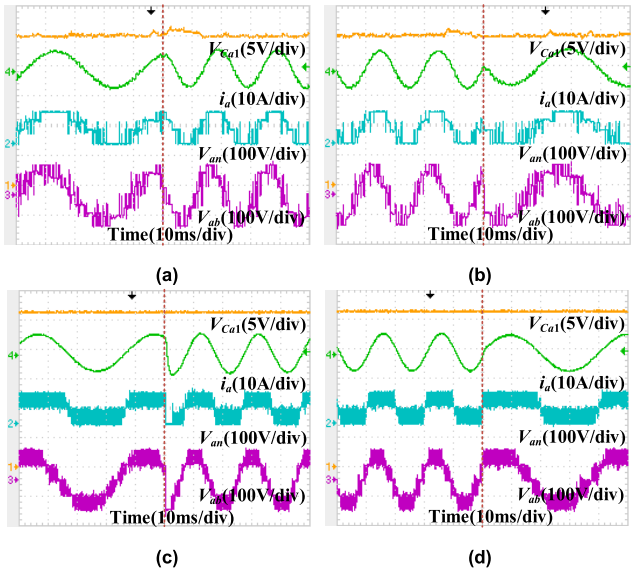

FIGURE 20. Dynamic results of the MPC and ICO-PWM method under changing current frequency. (a)/(c) MPC /ICO-PWM under the current frequency changing from 50 to 100 Hz, (b)/(d) MPC /ICO-PWM under the current frequency changing from 100 to 50 Hz.

can be selected. Therefore, it has great practical significance for industrial applications of the T-NNPC topology.

VII. CONCLUSION

This paper proposes an ICO-PWM method for an attractive T-NNPC topology, applied to medium-voltage applications, controlling the flying capacitor voltage better. Firstly, the proposed ICO-PWM is achieved by expanding the voltage level distribution in the vertical direction based on the conventional CO-PWM, improving the voltage level contents for controlling the flying capacitors under the high modulation indexes and achieving good five-level output. Secondly, the proposed ICO-PWM improves the stability of flying capacitor voltage control under low-frequency conditions, reduces the flying capacitor voltage deviation by more than five times, and improves the performance of output current. Finally, the performance of the proposed method is verified in simulations and experiments, respectively.

REFERENCES

[1] J. Rodriguez, J.-S. Lai, and F. Z. Peng, "Multilevel inverters: A survey of topologies, controls, and applications," *IEEE Trans. Ind. Electron.*, vol. 49, no. 4, pp. 724–738, Aug. 2002.

[2] K. K. Gupta, A. Ranjan, P. Bhatnagar, L. K. Sahu, and S. Jain, "Multilevel inverter topologies with reduced device count: A review," *IEEE Trans. Power Electron.*, vol. 31, no. 1, pp. 135–151, Jan. 2016.

[3] M. D. Siddique, S. Mekhilef, N. M. Shah, and M. A. Memon, "Optimal design of a new cascaded multilevel inverter topology with reduced switch count," *IEEE Access*, vol. 7, pp. 24498–24510, 2019.

[4] Y. Yu, X. Li, and L. Wei, "Fault tolerant control of five-level inverter based on redundancy space vector optimization and topology reconfiguration," *IEEE Access*, vol. 8, pp. 194342–194350, 2020.

[5] J. Ebrahimi, S. Eren, and A. Bakhshai, "Capacitor voltages balancing method for flying capacitor multilevel converters based on overall priority index," in *Proc. IEEE 14th Int. Conf. Power Electron. Drive Syst. (PEDS)*, Aug. 2023, pp. 1–6.

[6] M.-K. Nguyen and T.-T. Tran, "Quasi cascaded H-bridge five-level boost inverter," *IEEE Trans. Ind. Electron.*, vol. 64, no. 11, pp. 8525–8533, Nov. 2017.

[7] A. Bahrami and M. Narimani, "A new five-level T-type nested neutral point clamped (T-NNPC) converter," *IEEE Trans. Power Electron.*, vol. 34, no. 11, pp. 10534–10545, Nov. 2019.

[8] K. Wang, L. Xu, Z. Zheng, and Y. Li, "Capacitor voltage balancing of a five-level ANPC converter using phase-shifted PWM," *IEEE Trans. Power Electron.*, vol. 30, no. 3, pp. 1147–1156, Mar. 2015.

[9] E. Burguete, J. López, and M. Zabaleta, "New five-level active neutral-point-clamped converter," *IEEE Trans. Ind. Appl.*, vol. 51, no. 1, pp. 440–447, Jan. 2015.

[10] H. Wang, L. Kou, Y.-F. Liu, and P. C. Sen, "A seven-switch five-level active-neutral-point-clamped converter and its optimal modulation strategy," *IEEE Trans. Power Electron.*, vol. 32, no. 7, pp. 5146–5161, Jul. 2017.

[11] A. Dekka and M. Narimani, "Capacitor voltage balancing and current control of a five-level nested neutral-point-clamped converter," *IEEE Trans. Power Electron.*, vol. 33, no. 12, pp. 10169–10177, Dec. 2018.

[12] J. Ebrahimi, H. Karshenas, S. Eren, and A. Bakhshai, "An optimized capacitor voltage balancing control for a five-level nested neutral point clamped converter," *IEEE Trans. Power Electron.*, vol. 36, no. 2, pp. 2154–2165, Feb. 2021.

[13] M. Narimani, B. Wu, and N. R. Zargari, "A novel five-level voltage source inverter with sinusoidal pulse width modulator for medium-voltage applications," *IEEE Trans. Power Electron.*, vol. 31, no. 3, pp. 1959–1967, Mar. 2016.

[14] K. Wang, Z. Zheng, L. Xu, and Y. Li, "Topology and control of a five-level hybrid-clamped converter for medium-voltage high-power conversions," *IEEE Trans. Power Electron.*, vol. 33, no. 6, pp. 4690–4702, Jun. 2018.

[15] H. Wang, L. Kou, Y.-F. Liu, and P. C. Sen, "A new six-switch five-level active neutral point clamped inverter for PV applications," *IEEE Trans. Power Electron.*, vol. 32, no. 9, pp. 6700–6715, Sep. 2017.

[16] Y. P. Siwakoti, A. Palanisamy, A. Mahajan, S. Liese, T. Long, and F. Blaabjerg, "Analysis and design of a novel six-switch five-level active boost neutral point clamped inverter," *IEEE Trans. Ind. Electron.*, vol. 67, no. 12, pp. 10485–10496, Dec. 2020.

[17] C. Rech and W. A. P. Castiblanco, "Five-level switched-capacitor ANPC inverter with output voltage boosting capability," *IEEE Trans. Ind. Electron.*, vol. 70, no. 1, pp. 29–38, Jan. 2023.

[18] R. Barzegarkhoo, M. Farhangi, S. S. Lee, R. P. Aguilera, M. Liserre, and Y. P. Siwakoti, "New family of dual-mode active neutral point-clamped five-level converters," *IEEE Trans. Power Electron.*, vol. 30, no. 10, pp. 12236–12253, Oct. 2023.

[19] K. Wang, Z. Zheng, L. Xu, and Y. Li, "An optimized carrier-based PWM method and voltage balancing control for five-level ANPC converters," *IEEE Trans. Ind. Electron.*, vol. 67, no. 11, pp. 9120–9132, Nov. 2020.
[20] T. B. Hashfi, S. Mekhilef, M. Mubin, M. Seyedmahmoudian, B. Horan, and A. Stojcevski, "Adaptive carrier-based PDPWM control for modular multilevel converter with fault-tolerant capability," *IEEE Access*, vol. 8, pp. 26739–26748, 2020.
[21] Y. Yang, H. Wen, M. Fan, M. Xie, S. Peng, M. Norambuena, and J. Rodriguez, "Computation-efficient model predictive control with common-mode voltage elimination for five-level ANPC converters," *IEEE Trans. Transport. Electrific.*, vol. 6, no. 3, pp. 970–984, Sep. 2020.
[22] V. Srinath, M. Agarwal, and D. K. Chaturvedi, "Simulation and design of modified SPWM and single-phase five-level inverter," in *Proc. IEEE 15th Int. Conf. Ind. Inf. Syst. (ICIIS)*, Nov. 2020, pp. 1–6.
[23] C. Liu, C. Du, X. Xing, Y. Jiang, R. Zhang, X. Li, and C. Zhang, "Leakage current suppression of transformerless 5L-ANPC inverter with lower ripple model predictive control," *IEEE Trans. Ind. Appl.*, vol. 58, no. 5, pp. 6297–6309, Sep. 2022.

HUA CHEN was born in China, in 1985. She received the B.S. and M.S. degrees from Qufu Normal University, Jining, China, in 2009 and 2012, respectively.

She is currently a Lecturer with Shandong Labor Vocational and Technical College, Jinan, Shandong, China. Her current research interests include parallel inverters systems, power conversion, and renewable power generation.

CHUANGPING WEN was born in Fujian, China, in 1999. He received the B.S. degree in electrical engineering and automation from Shandong University, Jinan, China, in 2021, where he is currently pursuing the M.S. degree in electrical engineering with the School of Control Science and Engineering.

His current research interests include topologies and control strategies of multilevel inverters.

ZUOHANG HU was born in Shandong, China, in 1999. He received the B.S. degree in automation from Shandong University, Jinan, China, in 2022, where he is currently pursuing the M.S. degree in electrical engineering with the School of Control Science and Engineering.

His current research interests include power quality management and control strategies of multilevel inverters.

XIANGYANG XING (Member, IEEE) received the B.S. degree in automation and the M.S. degree in control theory and application from Qufu Normal University, China, in 2009 and 2012, and the Ph.D. degree in electrical engineering from Shandong University, Jinan, China, in 2016.

In 2019, he joined Shandong University, where he is currently a Professor with the School of Control Science and Engineering. His current research interests include multilevel converters and power conversion.